Efficiency enhancement in waste heat recovery ORC plants by means of reheating

Ana Ortega-Sarceda[a], Alberto Arce[b], Alberto Benato[c, CA] and Giovanna Cavazzini[d]

[a] *CITENI, Campus Industrial de Ferrol, Universidade da Coruña, Ferrol, Spain, ana.ortega@udc.es*
[b] *CITENI, Campus Industrial de Ferrol, Universidade da Coruña, Ferrol, Spain, alberto.arce@udc.es*
[c] *Department of Industrial Engineering, University of Padova, Padova, Italy, alberto.benato@unipd.it, CA*
[d] *Department of Industrial Engineering, University of Padova, Padova, Italy, giovanna.cavazzini@unipd.it*

Abstract:

The increasing global energy demand and environmental concerns have intensified the need for efficient waste heat recovery technologies. Organic Rankine Cycles (ORCs) are widely used for converting low-grade thermal energy into power; however, their performance strongly depends on both the working fluid and cycle configuration. In this study, a reheat-regenerative ORC (RR-ORC) is analysed and optimized to enhance energy recovery from low-temperature heat sources. A Multi-System Particle Swarm Optimization (MS-PSO) approach is employed to simultaneously evaluate multiple working fluids while preserving their individual thermodynamic constraints. Five representative fluids—Isobutane, Pentane, cis-2-butene, R245fa, and R1336mzz(Z)—are considered. The optimization framework maximizes thermal efficiency by tuning key operating variables, including pump outlet pressure, expander inlet temperature, reheating pressure and temperature, condenser conditions, and pinch-point temperature differences. The results show that the proposed MS-PSO method ensures stable convergence and enables consistent comparison among working fluids. Scenario analysis reveals that a configuration with high cognitive and social coefficients and low inertia weight provides the best optimization performance. Among the evaluated fluids, cis-2-butene achieves the highest thermal efficiency (19.36%), as well as superior exergetic efficiency (57.27%) and specific net power output (97.80 kJ/kg). A sensitivity analysis indicates that the most influential operating parameters depend strongly on the selected working fluid, with expander inlet temperature, reheating temperature, and pump outlet pressure playing dominant roles. Additionally, an economic assessment based on heat exchanger design highlights the trade-off between thermodynamic performance and system cost. Overall, the optimized RR-ORC configuration demonstrates improved thermo-economic performance, supporting its potential for efficient and cost-effective low-grade waste heat recovery.

Keywords:

Energy; PSO; Reheat-Regenerative ORC; Thermal Efficiency; Waste Heat Recovery.

1. Introduction

Growing global energy demand, together with increasing environmental concerns, is driving the development of more efficient and sustainable energy conversion technologies. In many industrial sectors, a significant share of the supplied energy is still rejected as medium- and low-temperature waste heat, resulting in reduced overall efficiency and unnecessary emissions. Therefore, the recovery and effective utilization of waste thermal energy represent an important strategy for improving process sustainability and reducing primary energy consumption [1].

Previous studies [2, 3] have shown that the thermophysical properties of the working fluid (WF), such as critical temperature and molecular structure, strongly affect the thermal and exergetic performance of Organic Rankine Cycles (ORCs). For this reason, parametric thermodynamic analyses have been widely adopted to identify suitable operating conditions for different working fluids (WFs) [4]. In this context, Rad *et al.* [5] pointed out that the optimal fluid selection is closely related to the match between the heat-source temperature and the fluid critical temperature. On this basis, the present study considers Isobutane, Pentane, cis-2-butene, R245fa, and R1336mzz(Z), representing hydrocarbon, hydrofluorocarbon, and hydrofluoroolefin families.

In addition to working-fluid selection, several studies have investigated system-level modifications aimed at enhancing ORC performance. Pei *et al.* [6], for example, showed that the adoption of an internal heat exchanger (IHX) can increase thermal efficiency by about 5%. Similarly, Liao *et al.* [7], through combined energy and exergy analyses, found that regenerative ORC configurations generally outperform simple cycles

by preheating the WF with the IHX. Using a genetic algorithm (GA), Gimelli *et al.* [8] optimized a regenerative ORC layout and reported a thermal efficiency of 18.9%.

Other contributions have focused on the influence of operating parameters and more advanced cycle architectures. Hemadri and Subbarao [9] investigated the effects of reheating pressure and turbine inlet temperature on mass flow rate and cycle efficiency. Di Genova *et al.* [10] analyzed reheat-regenerative ORC (RR-ORC) configurations with multiple reheating stages, assuming a constant pinch-point temperature difference of 10 K. Since this parameter has a strong impact on both heat-exchanger sizing and cycle performance, it is treated as an optimization variable in the present work.

In parallel, metaheuristic optimization techniques have gained increasing attention in ORC research due to their ability to efficiently explore complex multidimensional design spaces with relatively low computational cost. Among these methods, Particle Swarm Optimization (PSO) has shown particularly promising performance, often outperforming genetic algorithms in the search for optimal ORC configurations. For instance, Bornatico *et al.* [11] reported faster convergence and improved optimization results when applying PSO to a solar thermal building system, while Chagnon-Lessard and Gosselin [12] used PSO to optimize the heat cascade in an ORC. However, PSO performance is strongly influenced by the choice of its control parameters, namely the inertia weight and the cognitive and social coefficients, which govern the balance between exploration and exploitation. Inappropriate parameter settings may lead to premature convergence or excessive computational effort [13]. Moreover, in many existing approaches, the optimization is performed for one WF at a time, which increases the overall computational burden.

Although previous studies have investigated working-fluid selection, advanced ORC layouts, and PSO-based optimization, these aspects have often been addressed separately. In particular, limited attention has been devoted to the simultaneous optimization of multiple WFs in reheat-regenerative ORC (RR-ORC) systems while preserving fluid-specific feasibility constraints. In many existing approaches, each WF is optimized independently, which increases computational effort and may limit the consistency of the comparison among candidate fluids. Moreover, despite the recognized importance of PSO parameter tuning, its influence on the optimization of RR-ORC systems with different WFs has not yet been sufficiently clarified.

To address these gaps, the present study adopts a modified particle swarm optimization strategy, referred to as Multi-System PSO (MS-PSO), which maintains independent feasible search domains for each WF while enabling their simultaneous evaluation within a unified optimization framework. In this way, the proposed approach combines three main elements of novelty: first, it extends PSO-based optimization to the multi-fluid assessment of a RR-ORC configuration with superheating; second, it explicitly investigates the sensitivity of the optimization results to the PSO control parameters; third, unlike previous RR-ORC studies assuming a fixed pinch-point temperature difference, it includes this parameter among the decision variables, thereby accounting more realistically for its effect on both cycle performance and heat-exchanger sizing. In addition, an economic analysis based on the thermal design of the system is performed to identify ORC solutions that are not only thermodynamically efficient, but also economically viable.

The remainder of this manuscript is organized as follows. Section 2 describes the RR-ORC layout and the thermodynamic model and the optimization methodology, including the MS-PSO approach and the selected decision variables. Section 3 discusses the results of the parametric and sensitivity analyses, together with the comparison among the considered WFs. Finally, Section 4 summarizes the main findings and draws the conclusions of the study.

2. Methodology

This section describes the methodological framework adopted in the present study. First, the RR-ORC system configuration is introduced. Then, the thermodynamic and economic models are presented, followed by the formulation of the optimization problem. Finally, the Multi-System Particle Swarm Optimization (MS-PSO) approach and the corresponding computational settings are described.

2.1. RR-ORC system description

The system investigated in this work is a reheat-regenerative Organic Rankine Cycle (RR-ORC) for waste heat recovery. The plant converts thermal energy into electricity through eight thermodynamic states, as shown in Figure 1. The main processes are: first-stage expansion in the high-pressure turbine (1–2), reheating (2–3), second-stage expansion in the low-pressure turbine (3–4), precooling in the regenerator (4–5), condensation (5–6), pumping (6–7), preheating in the regenerator (7–8), and evaporation and superheating in the evaporator (8–1).

A constant mass flow of the heat-transfer fluid (HTF), Therminol VP1, enters the evaporator and reheater at T_{hs} = 200ºC, while cooling water enters the condenser at T_{cs} = 25ºC, in agreement with values commonly adopted in the literature [14]. Five candidate WFs are considered within the optimization framework, namely Isobutane, Pentane, cis-2-butene, R245fa, and R1336mzz(Z). These fluids are representative of low- to medium-temperature ORC applications and provide a suitable balance between thermophysical performance, operational feasibility, and environmental acceptability. Their main physical, safety, and environmental

properties are summarized in Table 1. Figure 1 illustrates the RR-ORC configuration by means of the schematic layout, the corresponding T-s diagram, and the T-Q diagram of the evaporator.

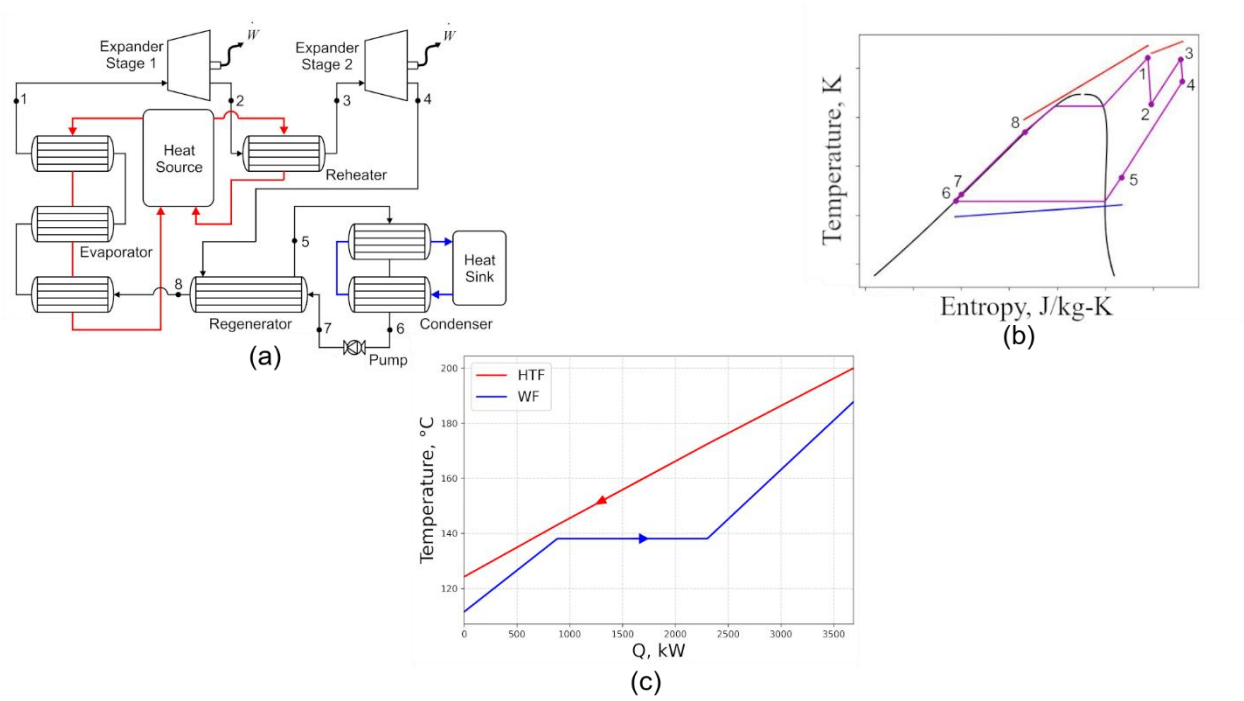

Figure. 1. *(a)Schematic diagram, (b) T-s diagram, (c) T-Q diagram of the evaporator for the RR-ORC.*

Table 1. *Physical, safety and environmental data of the selected fluids.*

Fluid	Physical properties				Safety data[a]	Env. Data	
	MM, g/mol	T_{bp}, °C	T_{cr}, °C	P_{cr}, kPa		ODP	GWP
Isobutane [15]	58.12	-11.7	134.7	3629	A3	0	~20
Pentane [15]	72.15	36.1	196.6	3368	A3	0	~20
Cis-2-butene [16, 17]	56.11	3.72	162.6	4226	—	0	2
R245fa [15]	134.05	15.1	153.86	3651	B1	0	1050
R1336mzz(Z) [18]	164.06	33.45	171.35	2903	A1	0	2

[a] Safety classification: A=lower toxicity; B=higher toxicity; 1=no flame propagation; 2=lower flammability; 3=higher flammability.

2.2. Thermodynamic and economic model

The RR-ORC system is analysed under steady-state conditions by means of a thermodynamic model based on the First and Second Laws of Thermodynamics, coupled with an economic assessment of the main components. Heat losses to the surroundings are neglected, as are variations in kinetic and potential energy. In addition, chemical exergy is not taken into account according to Wang *et al.* [19].

The thermophysical properties of the WFs are evaluated using REFPROP [20], while those of the heat-transfer fluid are obtained from CoolProp [21]. The operating and economic input parameters adopted in the simulations are listed in Table 2.

Table 2. *Operating conditions and economic input parameters.*

Parameter and unit	Value	Reference
HTF mass flow rate, kg/s	25	[22]
Maximum cooling water outlet temperature, °C	40	[23]
Expander isentropic efficiency, %	85	[24]
Pump isentropic efficiency, %	85	[25]
The operating time, h	8000	[26]
Life cycle time, yr	20	[26]
Annual loan interest rate	0.05	[26]
Grid electric price, $/MWh	150	[26]

The economic model is based on the methodology proposed by Zhang *et al.* [26] and the payback period (PP) is also evaluated. Heat-transfer coefficients are calculated by applying the Taborek formulation of the Bell–Delaware method for shell-side heat transfer [27, 28], whereas the Gnielinski correlation is used for the tube side [29]. For phase-change heat transfer, the Gungor–Winterton correlation [30, 31] and the Shah correlation [32] are employed. Pressure drops are estimated according to the correlations reported by Zhang *et al.* [26].

This modelling framework allows the evaluation of thermal and exergetic performance indicators together with heat-exchanger sizing and the corresponding economic implications, thus providing a consistent basis for the subsequent optimization.

2.3. Optimization problem formulation

The optimization objective is to maximize the thermal efficiency of the RR-ORC system, whose expression is given below:

$$\eta_I = \frac{W_n}{Q_{in}}, \qquad (1)$$

To this end, the optimization problem is formulated by selecting eight operating variables that govern the thermodynamic behaviour of the cycle:

- pump outlet pressure, P_7, which affects the heat-addition process;
- first expander inlet temperature, T_1, which determines the superheating level before the first expansion;
- reheating pressure, P_2, which defines the intermediate pressure level between the two expansion stages;
- second expander inlet temperature, T_3, which sets the reheating level before the second expansion stage;
- second expander outlet pressure, P_4, which influences the end of the second expansion process and affects both net power output and condensation conditions;
- condenser inlet temperature, T_5, which determines the thermal state of the WF entering the condenser and affects heat recovery in the regenerator;
- evaporator pinch-point temperature difference, ΔT_{pe}, which influences both thermal feasibility and heat-exchanger area;
- condenser pinch-point temperature difference, ΔT_{pc}, which plays an analogous role on the cold side.

Operational and thermodynamic constraints are imposed to ensure physically feasible and stable cycle operation. In particular, the condensation pressure is maintained above atmospheric pressure in order to avoid vacuum conditions, while the evaporation pressure is kept below the critical pressure to guarantee subcritical operation. Moreover, ΔT_p in both the evaporator and the condenser are constrained within the range of 5–10 K. The optimization problem is solved independently for each WF, while maintaining a common formulation in terms of objective function, decision variables, and algorithmic settings.

2.4. Multi-System PSO approach

Particle Swarm Optimization (PSO) is a stochastic population-based optimization method inspired by the collective behaviour of natural swarms [33, 34, 35]. In PSO, each particle represents a candidate solution and moves within the search space according to its own experience and the information shared by the swarm, progressively converging toward promising regions.

In the present work, a Multi-System PSO (MS-PSO) strategy is adopted in order to extend the conventional PSO framework to a multi-fluid optimization problem. The main rationale for this choice is that each WF is characterized by different thermodynamic limits and feasibility constraints. As a consequence, the direct use of a single global best solution for all fluids may drive some particles toward regions of the search space that are not admissible for the corresponding fluid.

To overcome this limitation, the proposed MS-PSO framework assigns an independent swarm to each WF. In this way, each subsystem explores only its own feasible domain, and information exchange is restricted to particles belonging to the same fluid-specific swarm. At the same time, identical PSO control parameters are adopted for all subsystems in order to ensure methodological consistency and enable a fair comparison among the candidate fluids.

This strategy makes it possible to evaluate multiple fluids within a unified optimization framework while preserving fluid-specific admissibility conditions and avoiding cross-fluid convergence toward infeasible solutions.

2.5. PSO settings and computational procedure

In each swarm, the particle velocity and position are iteratively updated according to the standard PSO equations:

$$v_i(t+1) = \omega \cdot v_i(t) + c_1 \cdot rand_1 \cdot (p_i(t) - x_i(t)) + c_2 \cdot rand_2 \cdot (g(t) - x_i(t)), \qquad (2)$$

$$x_i(t+1) = x_i(t) + v_i(t+1), \qquad (3)$$

where v_i is the particle velocity, x_i is the particle position, p_i is the personal best position, g is the best position identified by the swarm, ω is the inertia weight, and c_1 and c_2 are the cognitive and social acceleration coefficients, respectively.

According to the ranges suggested in the literature, the inertia weight is selected within ($0.5 < \omega < 1$), while the acceleration coefficients satisfy ($c_1 + c_2 < 4$) [36, 37, 38]. The PSO algorithm is implemented using 20 particles [38] and a maximum of 1000 iterations [12]. To investigate the influence of the control parameters on the optimization performance, nine different hyperparameter scenarios are considered by combining three values of c_1=c_2 and three values of ω, as reported in Table 3. Each scenario is executed ten times for each WF, and the reported results correspond to the average of the best thermal efficiencies obtained over the ten runs.

Table 3. *PSO hyperparameter values considered in the sensitivity analysis.*

Scenarios	Hyperparameter values	
	c_1, c_2	ω
1	1.000 [40]	0.5000 [41]
2	1.000 [40]	0.7298 [42]
3	1.000 [40]	0.8000 [43]
4	1.496 [12]	0.5000 [41]
5	1.496 [12]	0.7298 [42]
6	1.496 [12]	0.8000 [43]
7	2.000 [44]	0.5000 [41]
8	2.000 [44]	0.7298 [42]
9	2.000 [44]	0.8000 [43]

3. Results and discussion

This section presents and discusses the main outcomes of the optimization analysis. First, the effect of the PSO hyperparameters on the optimization performance is examined to identify the most suitable parameter combination for the considered RR-ORC problem. Then, the optimized thermodynamic performance of the selected WFs is compared. The corresponding optimal operating conditions are subsequently analysed in order to clarify the physical reasons behind the observed trends. Finally, the economic performance of the optimal solutions is assessed, and the main results are discussed in light of the available literature.

3.1. Effect of PSO hyperparameters on optimization performance

Table 4 reports the thermal efficiencies obtained for the nine PSO hyperparameter scenarios considered in this study, for each of the selected WFs. The results show that the choice of the PSO control parameters has a noticeable effect on the optimization outcome, although the magnitude of this effect depends on the WF.

Table 4. *Thermal efficiency per scenario and WF.*

Scenarios	WF				
	Isobutane	Pentane	Cis-Butene	R245fa	R1336mzz(Z)
1	16.86	16.63	18.37	16.88	15.20
2	17.52	17.17	18.78	17.13	15.20
3	17.51	17.05	18.38	17.17	15.55
4	17.73	17.81	19.23	17.43	15.66
5	17.29	17.68	18.62	17.25	15.68
6	17.20	17.49	18.31	16.71	15.46
7	17.60	17.85	19.36	17.49	16.00
8	16.60	16.63	18.20	16.64	15.31
9	16.62	16.81	18.03	16.32	15.21

For Pentane, cis-2-butene, R245fa, and R1336mzz(Z), the highest thermal efficiency is obtained under Scenario 7, corresponding to c_1=c_2=2.0 and ω=0.5. This result suggests that, for these fluids, a relatively strong attraction toward the personal and swarm best positions combined with a limited inertia term provides an effective balance between exploration and exploitation, thus favouring convergence toward high-quality solutions. By contrast, Isobutane achieves its maximum thermal efficiency under Scenario 4, while Scenario 7 yields a slightly lower value. This indicates that the most suitable hyperparameter combination is not identical for all fluids, and that the optimization performance remains dependent on the characteristics of the corresponding feasible search domain.

A comparison among the scenarios also highlights some general trends. For most fluids, the best results are obtained when relatively high values of the acceleration coefficients are adopted. In addition, lower inertia weights appear to be more effective than higher ones, as scenarios with ω=0.8 generally lead to lower thermal

efficiencies. This behaviour can be attributed to the fact that an excessively large inertia term may favour exploration at the expense of convergence, thereby reducing the algorithm's ability to refine the search around promising regions of the solution space.

Overall, the results confirm that PSO tuning plays a relevant role in the optimization of RR-ORC systems. Although Scenario 7 can be regarded as the most suitable general configuration for the present application, the behaviour observed for Isobutane suggests that fluid-specific differences should also be taken into account when interpreting the optimization performance. On this basis, Scenario 7 is selected as the reference case for the subsequent comparison of the thermodynamic performance of the investigated WFs, while the deviation observed for Isobutane is discussed in relation to its optimal operating conditions in the following sections.

3.2. Optimal thermodynamic performance of the selected working fluids

Table 5 summarizes the main performance indicators obtained for the optimal scenario for each WF. Overall, the results show that the selected fluids exhibit markedly different thermodynamic and thermo-economic behaviours, confirming the importance of working-fluid selection in RR-ORC applications.

Among the investigated candidates, cis-2-butene provides the best overall thermodynamic performance. It achieves the highest thermal efficiency, equal to 19.36%, together with the highest exergy efficiency, 57.21%, and the highest specific net power output, 97.80 kJ/kg. These results indicate that cis-2-butene is the most effective fluid for exploiting the available heat source under the considered operating conditions.

Table 5. *Performance indicators of the WFs for optimal scenario.*

Performance	WF				
Indicator	Isobutane	Pentane	Cis-Butene	R245fa	R1336mzz(Z)
η_I, %	17.60	17.85	19.36	17.49	16.00
η_{II}, %	53.26	49.61	57.21	52.55	46.19
w_{net}, kJ/kg	74.11	83.83	97.80	42.99	34.16
e_d, kJ/kg	56.60	69.76	63.01	31.47	32.93
m_{WF}, kg/s	10.83	4.654	7.812	17.21	14.24
A, m^2	1389	479.9	1137	1168	626.8
PP, yr	2.880	3.048	2.530	2.812	2.844

Pentane and Isobutane also show competitive thermal efficiencies, equal to 17.85% and 17.60%, respectively, although their behaviour differs in terms of exergy efficiency, specific net power output, and required mass flow rate. Pentane reaches the second-highest thermal efficiency and a relatively high specific net work, whereas Isobutane combines good thermodynamic performance with a shorter payback period, despite requiring a larger heat-transfer area.

R245fa and R1336mzz(Z) exhibit lower thermal efficiencies, equal to 17.49% and 16.00%, respectively. R245fa maintains a relatively high exergy efficiency despite its lower specific net work, whereas R1336mzz(Z) shows the lowest thermal and exergy efficiencies among the selected fluids. This suggests that, for the present RR-ORC application, these two fluids are less effective than the hydrocarbon-based candidates and cis-2-butene in converting the available waste heat into useful power.

The specific exergy destruction rate follows a different trend from the efficiency indicators. In particular, the lowest values are obtained for R245fa and R1336mzz(Z), which also have the highest working-fluid mass flow rates. This behaviour indicates that the ranking based on exergy destruction does not directly coincide with that based on cycle efficiency, and that the comparison among fluids should account for multiple performance indicators.

A further trade-off emerges when considering the heat-transfer area and the payback period. In general, larger heat-transfer areas are associated with improved power generation and, consequently, shorter payback periods. In this respect, cis-2-butene appears especially attractive, as it combines the highest thermodynamic performance with the shortest payback period, equal to 2.530 years. By contrast, Pentane requires the smallest heat-transfer area, 479.9 m^2, but exhibits the longest payback period, equal to 3.048 years.

Overall, the results identify cis-2-butene as the most promising WF for the considered RR-ORC system, owing to its superior thermal and exergetic performance as well as its favourable economic response. However, the different trends observed for the other fluids indicate that the final ranking depends on the selected performance indicator. For this reason, a more detailed analysis of the optimal operating conditions is required in order to clarify the physical reasons behind the observed differences among the investigated fluids.

3.3. Sensitivity of thermal efficiency to the operating variables

Figures 2–6 provide further insight into the influence of the decision variables on the thermal efficiency of the RR-ORC system for the investigated WFs. Overall, the results confirm that the relative importance of the

operating variables is strongly fluid-dependent, reflecting the different thermodynamic characteristics of the candidate fluids and their different responses to pressure and temperature variations within the cycle.

For Isobutane, Figure 2 shows that Scenario 4 yields the highest thermal efficiency. This scenario is characterized by high values of P_7, T_1, and P_2, intermediate values of T_3, and low values of P_4 and T_5. A comparison with Scenario 7 suggests that Isobutane is more sensitive to the inlet temperatures T_1 and T_3 than to the pump outlet pressure P_7. Moreover, the comparison between Scenarios 2 and 3 indicates that moderate changes in P_4 and T_5 have only a limited effect on thermal efficiency. Therefore, for Isobutane, the most influential variables are T_1 and T_3, followed by P_7, while P_4, T_5, and P_2 appear to play a secondary role.

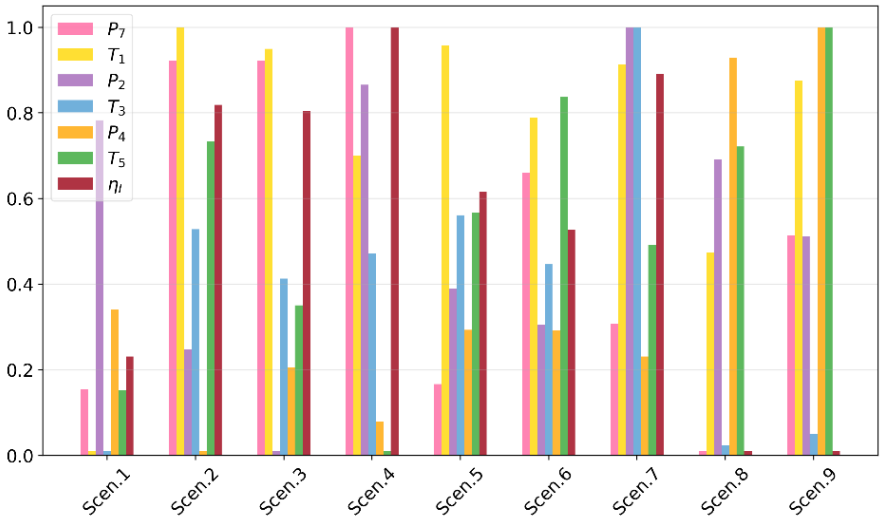

Figure. 2. *Normalized thermal efficiency of Isobutane.*

For Pentane, Figure 3 indicates that the highest thermal efficiency is obtained in Scenario 7, corresponding to high values of T_1, P_2, and T_3, intermediate values of P_7, and low values of P_4 and T_5. Scenario 4 also leads to a relatively high thermal efficiency, despite a different combination of pressure levels, namely higher P_7 and lower P_4 and T_5, which implies a greater expansion ratio. However, the lower values of T_1 and T_3 in this case limit the achievable efficiency. This behaviour indicates that, for Pentane, the turbine inlet temperatures T_1 and T_3 have a stronger effect on performance than the pressure-related variables P_7, P_2, and P_4, as well as T_5.

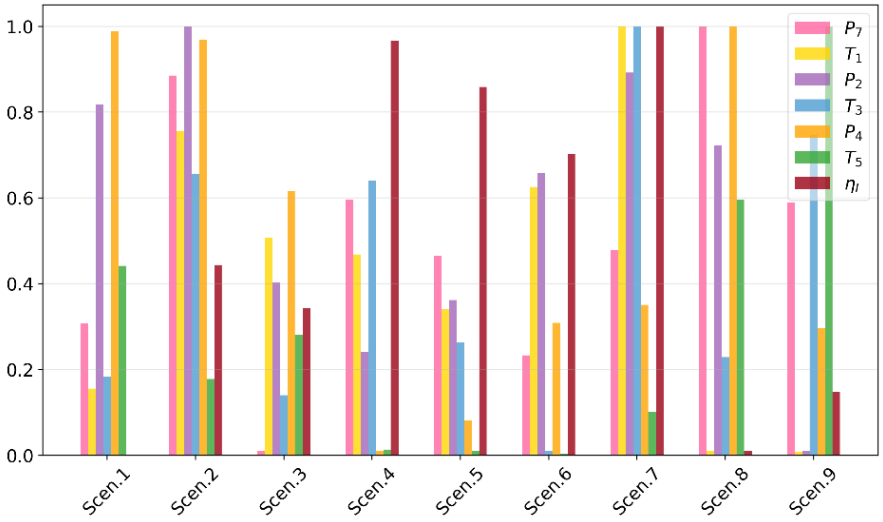

Figure. 3. *Normalized thermal efficiency of Pentane.*

A similar but not identical behaviour is observed for cis-2-butene. As shown in Figure 4, the maximum thermal efficiency is obtained under Scenario 7, with high P_7 and T_1, intermediate T_3, and low P_4 and T_5. Scenario 4, although characterized by higher P_7 and T_1 and minimum values of T_3, P_4, and T_5, results in a lower normalized thermal efficiency, mainly because of the low reheating temperature T_3. Conversely, operating at the minimum P_7, as in Scenario 2, causes a marked reduction in thermal efficiency even when T_1 and T_3 remain moderately high. The comparison between Scenarios 1 and 6 also highlights the influence of P_4, although its effect is less

pronounced than that of T_3. Overall, cis-2-butene appears to be mainly governed by P_7, followed by T_1 and T_3, whereas P_4 and the associated value of T_5 have a weaker influence.

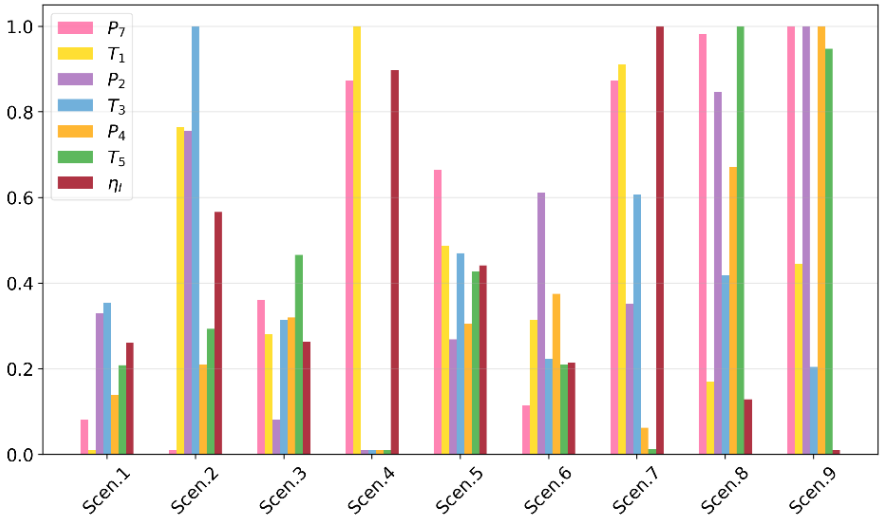

Figure. 4. *Normalized thermal efficiency of cis-Butene.*

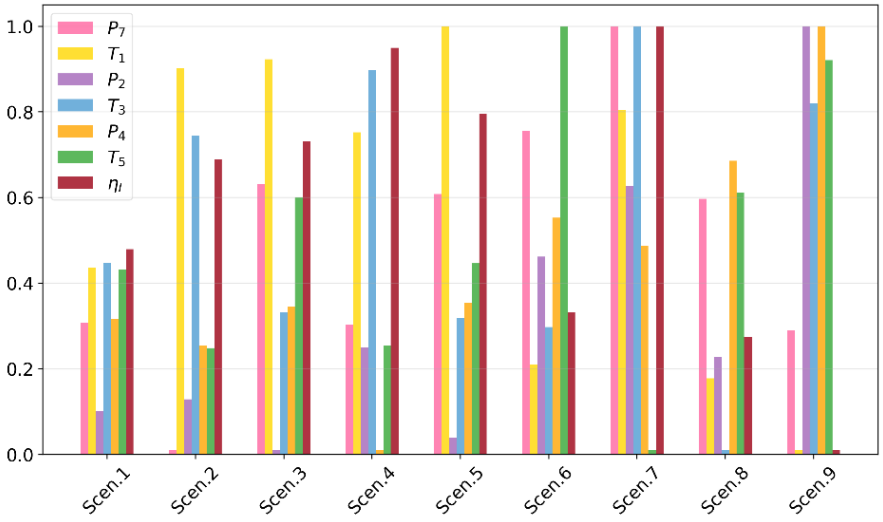

Figure. 5. *Normalized thermal efficiency of R245fa.*

For R245fa, Figure 5 shows that Scenario 7 again provides the highest thermal efficiency. This case is associated with high values of P_7 and T_1, intermediate values of P_2 and P_4, and low T_5. Scenario 4 operates with a lower normalized value of P_7 and the minimum P_4, resulting in lower overall expansion and a higher T_5, which leads to a lower thermal efficiency. A comparison between Scenarios 2 and 3 further indicates that P_7 has a stronger influence than T_5, since the higher P_7 in Scenario 3 compensates for the increase in condenser inlet temperature. In addition, T_1 has a major impact on system performance: when T_1 exceeds approximately 0.80 in normalized terms, the thermal efficiency remains relatively high, whereas lower values of T_1 are associated with a marked performance deterioration. Therefore, R245fa is mainly sensitive to T_1 and P_7, followed by T_5 and P_4, while the effect of T_3 appears less significant.

Finally, Figure 6 shows that R1336mzz(Z) reaches its maximum thermal efficiency in Scenario 7, characterized by high P_7, T_1, and P_2, intermediate T_3, and low P_4 and T_5. The comparison between Scenarios 1 and 2 suggests that the combined effect of P_7 and P_4 is comparable to the effect of T_5. In contrast with the behaviour observed for the other fluids, T_1 and T_3 appear to play a relatively minor role, as shown by Scenario 4, which yields lower efficiency than Scenario 5 despite higher values of both temperatures. This indicates that the performance of R1336mzz(Z) is governed primarily by pressure-related variables, especially P_7 and P_4, whereas T_5 has an intermediate influence and the two inlet temperatures remain secondary.

In summary, the analysis of the normalized thermal efficiencies highlights that no single operating variable dominates the system behaviour for all fluids. Instead, the relative importance of pressure levels and inlet temperatures depends strongly on the thermophysical properties of the WF. Hydrocarbon-based fluids and cis-2-butene tend to benefit more from higher turbine inlet temperatures and favourable pressure ratios,

whereas R1336mzz(Z) appears to be more strongly affected by pressure-related conditions. These differences help explain the ranking observed in Table 5 and confirm that the optimization of RR-ORC systems requires a fluid-specific analysis of the operating conditions.

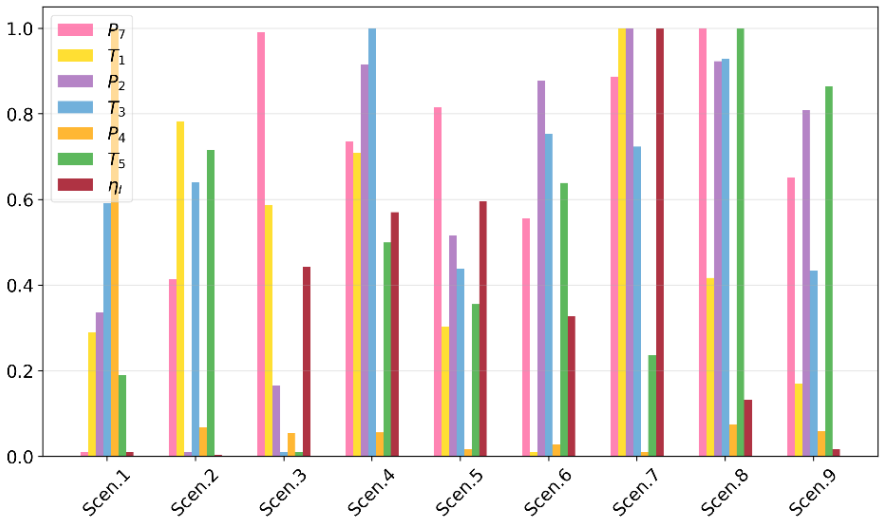

Figure. 6. *Normalized thermal efficiency of R1336mzz(Z).*

3.4. Economic performance, thermo-economic trade-offs, and comparison with literature

In addition to thermodynamic performance, the economic behaviour of optimized RR-ORC solutions plays a key role in the assessment of the most suitable WF. As shown in Table 5, the investigated fluids exhibit different trade-offs between efficiency, specific net power output, heat-transfer area, and payback period. These results confirm that the thermodynamically best solution does not necessarily correspond to the minimum investment cost, and that the final selection should account for both energy performance and economic viability.

Among the analysed fluids, cis-2-butene provides the most favourable overall compromise. In fact, it achieves not only the highest thermal and exergy efficiencies, but also the highest specific net power output and the shortest payback period, equal to 2.530 years. Although the corresponding heat-transfer area is relatively large, its superior power generation capability compensates for the higher capital cost, resulting in the most attractive economic response among the selected candidates.

A different behaviour is observed for Pentane. This fluid requires the smallest total heat-transfer area, equal to 479.9 m^2, which would normally be associated with a lower equipment cost. However, Pentane also exhibits the longest payback period, equal to 3.048 years. This result indicates that a reduced heat-transfer surface alone is not sufficient to ensure the best economic performance, since the payback period is also strongly influenced by the achievable power output and, consequently, by the annual economic return of the system.

Isobutane represents an intermediate case. Although its thermal efficiency is slightly lower than that of Pentane, it achieves a shorter payback period despite requiring a significantly larger heat-transfer area. This suggests that the higher energy performance of the optimized Isobutane-based cycle partly offsets the larger heat-exchanger cost. Similarly, R245fa and R1336mzz(Z) show less competitive thermodynamic performance, but their payback periods remain comparable to that of Isobutane, indicating that the overall economic ranking is influenced by the combined effect of efficiency, mass flow rate, and component sizing.

These results highlight the existence of a clear thermo-economic trade-off. On the one hand, larger heat-transfer areas generally improve heat recovery and power production, thus enhancing the economic return. On the other hand, they also imply higher investment costs. The final outcome therefore depends on the extent to which the gain in net power compensates for the increase in capital expenditure. In the present case, cis-2-butene proves to be the most advantageous solution because it combines high thermodynamic performance with a sufficiently strong economic return to offset the larger heat-transfer area.

From a broader perspective, the obtained thermal efficiencies are in line with the values typically reported in the literature for advanced ORC configurations operating with low- to medium-temperature heat sources. In particular, the optimized efficiencies obtained in this study are comparable to, or slightly higher than, the values reported for regenerative ORC systems, confirming the potential of the reheat-regenerative layout combined with suitable working-fluid selection and a dedicated optimization framework. Moreover, the present results highlight that the simultaneous multi-fluid MS-PSO approach can support not only the identification of the most efficient thermodynamic solution, but also the selection of configurations that remain attractive from an economic point of view.

Overall, the combined thermodynamic and economic analysis indicates that cis-2-butene is the most promising candidate for the investigated RR-ORC application. At the same time, the comparison among fluids confirms that the optimal choice cannot be based on a single indicator alone. Rather, a consistent assessment should simultaneously consider cycle efficiency, exergy performance, specific power output, component sizing, and economic return. These findings further support the usefulness of the proposed optimization framework for the design and comparative assessment of advanced ORC systems.

4. Conclusions

In this work, a reheat-regenerative Organic Rankine Cycle (RR-ORC) for low-grade waste heat recovery was investigated through thermodynamic modelling, economic assessment, and optimization using a Multi-System Particle Swarm Optimization (MS-PSO) framework. The proposed methodology enabled the simultaneous evaluation of multiple working fluids while preserving fluid-specific feasibility constraints, overcoming limitations associated with conventional single-fluid optimization approaches.

The results showed that PSO hyperparameters significantly affect the optimization outcome. In general, the best performance was obtained with high acceleration coefficients and low inertia weight. Scenario 7 (c_1=c_2=2.000, ω=0.5000) provided the best results for most WFs, while Isobutane achieved its optimum under Scenario 4, highlighting the importance of proper PSO tuning for RR-ORC optimization.

Among the investigated WFs, cis-2-butene exhibited the best overall performance, achieving the highest thermal efficiency (19.36%), exergy efficiency (57.21%), and specific net power output (97.80 kJ/kg). Pentane and Isobutane also showed competitive results, whereas R245fa and R1336mzz(Z) presented lower thermodynamic performance under the analysed conditions.

The analysis of the optimal operating conditions revealed that the influence of decision variables strongly depends on the WF. Turbine inlet temperatures and pressure levels were particularly important for hydrocarbons and cis-2-butene, while pressure-related variables had a greater impact on R1336mzz(Z). Economically, a trade-off between thermodynamic performance and component sizing was identified. Larger heat-transfer areas improved power production and reduced payback periods, although they increased investment costs. Cis-2-butene also achieved the best thermo-economic compromise, with the shortest payback period of 2.530 years.

Overall, the proposed MS-PSO framework proved to be an effective tool for the comparative optimization of RR-ORC systems considering multiple WFs and combined thermodynamic and economic criteria.

Acknowledgments

The author, Ana Ortega-Sarceda, would like to acknowledge the support from the Galician Government and the Ferrol Industrial Campus by means of the predoctoral research contract 2024/CP/189.

Nomenclature

Letter symbols

A	area, m^2
c_1	social acceleration coefficient
c_2	cognitive acceleration coefficient
e_d	specific exergy destruction rate, kJ/kg
ω	inertia coefficient
m_{WF}	mass flow rate, kg/s
P	pressure, kPa
PP	payback period, yr
Q	heat, kW
T	temperature, °C
W	power output, kW
w	specific power output, kJ/kg

Greek symbols

ΔT_p	pinch point temperature difference
η	efficiency

Subscripts and superscripts

bp	normal boiling point
c	condenser
cr	critical

cs cold source

e evaporator

hs hot source

I thermal

II exergetic

in input

n net

References

[1] Wang J., Dai Y., Gao L., Exergy analyses and parametric optimizations for different cogeneration power plants in cement industry. Appl. Energy 2009;86(6):941-948.

[2] Qiu G., Selection of working fluids for micro-CHP systems with ORC. Renew. Energy 2012;48:565-70.

[3] Zhao L., Bao J., Thermodynamic analysis of organic Rankine cycle using zeotropic mixtures. Appl. Energy 2014;130:748-56.

[4] Dai Y., Wang J., Gao L., Parametric optimization and comparative study of organic Rankine cycle (ORC) for low grade waste heat recovery. Energy Convers. Manag. 2009;50(3):576-82.

[5] Amiri Rad E., Maddah S., Mohammadi S., Simultaneous optimization of working fluid and boiler pressure in an organic Rankine cycle for different heat source temperatures. Energy 2020;194;116856.

[6] Pei G., Li J., Ji J., Analysis of low temperature solar thermal electric generation using regenerative Organic Rankine Cycle. Appl. Therm. Eng. 2010;30(8-9):998-1004.

[7] Liao G., E J., Zhang F., Chen J., Leng E., Advanced exergy analysis for Organic Rankine Cycle-based layout to recover waste heat of flue gas. Appl. Energy 2020;266;114891.

[8] Gimelli A., Luongo A., Muccillo M., Efficiency and cost optimization of a regenerative Organic Rankine Cycle power plant through the multi-objective approach. Appl. Therm. Eng. 2017;114:601-10.

[9] Hemadri V. B., Subbarao P. M. V., Thermal integration of reheated organic Rankine cycle (RH-ORC) with gas turbine exhaust for maximum power recovery. Therm. Sci. Eng. Prog. 2021;23;100876.

[10] DiGenova K. J., Botros B. B., Brisson J. G., Method for customizing an organic Rankine cycle to a complex heat source for efficient energy conversion, demonstrated on a Fischer Tropsch plant. Appl. Energy 2013;102:746-54.

[11] Bornatico R., Pfeiffer M., Witzig A., Guzzella L., Optimal sizing of a solar thermal building installation using particle swarm optimization. Energy 2012;41(1):31-7.

[12] Chagnon-Lessard N., Gosselin L., Heat cascade and heuristics to optimize ORC and identify the best internal configuration. Appl. Therm. Eng. 2023;233;121071.

[13] Chauhan D., Shivani, Suganthan P. N., Learning strategies for particle swarm optimizer: A critical review and performance analysis. Swarm Evol. Comput. 2025;98;102048.

[14] Hu B., Guo J., Effect of cooling water flow on heat transfer performance of horizontal tube spray falling film evaporator in ORC system. Energy Rep 2022;8:540–5.

[15] Zhang C., Liu C., Wang S., Xu X., Li Q., Thermo-economic comparison of subcritical organic Rankine cycle based on different heat exchanger configurations. Energy 2017;123:728-41.

[16] Zhou Y., Li S., Sun L., Zhao S., Ashraf Talesh S. S., Optimization and thermodynamic performance analysis of a power generation system based on geothermal flash and dual-pressure evaporation organic Rankine cycles using zeotropic mixtures. Energy 2020;194;116785.

[17] Rostamzadeh H., Ghaebi H., Vosoughi S., Jannatkhah J., Thermodynamic and thermoeconomic analysis and optimization of a novel dual-loop power/refrigeration cycle. Appl. Therm. Eng. 2018;138:1–17.

[18] Navarro-Esbrí J., Fernández-Moreno A., Mota-Babiloni A., Modelling and evaluation of a high-temperature heat pump two-stage cascade with refrigerant mixtures as a fossil fuel boiler alternative for industry decarbonization. Energy 2022;254;124308.

[19] Wang J., Sun Z., Dai Y., Ma S., Parametric optimization design for supercritical CO_2 power cycle using genetic algorithm and artificial neural network. Appl. Energy 2010;87(4):1317–24.

[20] Lemmon E.W., Bell I.H., Huber M.L., McLinden, M.O., NIST Standard Reference Database 23: Reference Fluid Thermodynamic and Transport Properties-REFPROP, Version 10.0, National Institute of Standards and Technology, Standard Reference Data Program;Gaithersburg;2018.

[21] Bell I. H., Wronski J., Quoilin S., Lemort, V., Pure and Pseudo-pure Fluid Thermophysical Property Evaluation and the Open-Source Thermophysical Property Library CoolProp. Ind Eng Chem Res 2014;53(6):2498–508.

[22] Xia J., Guo Y., Li Y., Wang J., Zhao P., Dai Y., Thermodynamic analysis and comparison study of two novel combined cooling and power systems with separators using CO2-based mixture for low grade heat source recovery. Energy Convers. Manag. 2020;215;112918.

[23] Zhao C., Zheng S., Zhang J., Zhang Y., Exergy and economic analysis of organic Rankine cycle hybrid system utilizing biogas and solar energy in rural area of China. Int J Green Energy 2017;14(14):1221–29.

[24] Holagh S. G., Haghghi M. A., Mohammadi Z., Chitsaz A., Exergoeconomic and environmental investigation of an innovative poly-generation plant driven by a solid oxide fuel cell for production of electricity, cooling, desalinated water, and hydrogen. Int. J. Energy Res. 2020;44(13):10126–54.

[25] Fan G., Gao Y., Ayed H., Marzouki R., Aryanfar Y., Jarad F., Guo, P., Energy and exergy and economic (3E) analysis of a two-stage organic Rankine cycle for single flash geothermal power plant exhaust exergy recovery. Case Stud. Therm. Eng. 2021;28;101554.

[26] Zhang C., Liu C., Xu X., Li Q., Wang S., Chen X., Effects of superheat and internal heat exchanger on thermo-economic performance of organic Rankine cycle based on fluid type and heat sources. Energy 2018;159:482–95.

[27] Kuppan T., Heat Exchanger Design Handbook. Boca Raton, USA: CRC Press; 2013.

[28] Taborek J., Shell-and-tube heat exchangers: single-phase flow. Heat Exchanger Design Handbook. New York, USA: Hemisphere Publishing Corporation; 1983.

[29] Gnielinski V., New equations for heat and mass transfer in turbulent pipe and channel flow. Int. Chem. Eng. 1976;16(2):359–67.

[30] Gungor K. E., Winterton R. H. S., Simplified general correlation for saturated flow boiling and comparisons of correlations with data. Chem. Eng. Res. Des. 1987;65:148–156.

[31] Lakew A. A., Bolland O., Working fluids for low-temperature heat source. Appl. Therm. Eng. 2010;30(10):1262–8.

[32] Shah M. M., A general correlation for heat transfer during film condensation inside pipes. Int. J. Heat. Mass. Transf. 1979;22(4):547–56.

[33] Fan S. K. S., Liang Y. C., Zahara E., A genetic algorithm and a particle swarm optimizer hybridized with Nelder–Mead simplex search. Comput. Ind. Eng. 2006;50(4):401-25.

[34] Eberhart R., Kennedy J., A new optimizer using particle swarm theory. MHS'95: Proceedings of the Sixth International Symposium on Micro Machine and Human Science; 1995 Oct 4-6; Nagoya, Japan. IEEE: 39-43.

[35] Shi Y., Eberhart R. C., Empirical study of particle swarm optimization. In: Proceedings of the 1999 Congress on Evolutionary Computation; 1999 July 6-9; Washington, DC, USA. IEEE:1945-50.

[36] Aydilek İ. B., Nacar M. A., GümüŞÇü A., Salur M. U., Comparing inertia weights of particle swarm optimization in multimodal functions. In: Proceedings of 2017 International Artificial Intelligence and Data Processing Symposium (IDAP); 2017 Sept 16-17; Malatya, Türkiye. IEEE: 1-5.

[37] Elbeltagi E., Hegazy T., Grierson D., Comparison among five evolutionary-based optimization algorithms. Adv. Eng. Inform. 2005;19(1):43-53.

[38] Zomaya A. Y., Handbook of Nature-inspired and Innovative Computing : Integrating Classical Models With Emerging Technologies. New York, USA: Springer; 2006.

[39] Cavazzini G., Bari S., Pavesi G., Ardizzon, G., A multi-fluid PSO-based algorithm for the search of the best performance of sub-critical Organic Rankine Cycles. Energy 2017;129:42–58.

[40] Sedighizadeh D., Masehian E., Particle Swarm Optimization Methods, Taxonomy and Applications. Int. J. Comput. Theory Eng. 2009;1(5):486-502.

[41] Mohan S., Dinesha P., Campana P. E., ANN-PSO aided selection of hydrocarbons as working fluid for low-temperature organic Rankine cycle and thermodynamic evaluation of optimal working fluid. Energy 2022;259;124968.

[42] He M., Liu M., Wang R., Jiang X., Liu B., Zhou H., Particle swarm optimization with damping factor and cooperative mechanism. Appl. Soft. Comput. 2019;76:45–52.

[43] Zhou J., Chu Y. T., Ren J., Shen W., He C., Integrating machine learning and mathematical programming for efficient optimization of operating conditions in organic Rankine cycle (ORC) based combined systems. Energy 2023;281;128218.

[44] Zhao M., Wei M., Song P., Liu Z., Tian G., Performance evaluation of a diesel engine integrated with ORC system. Appl. Therm. Eng. 2017;115:221–28.